CFD Letters

Journal homepage:
https://semarakilmu.com.my/journals/index.php/CFD_Letters/index
ISSN: 2180-1363

# Effects of the Conjugate Heat Transfer and Heat Flux Strength on the Thermal Characteristics of Impinging Jets

Ghassan Nasif[1,*], Yasser El-Okda[1] , Mouza Alzaabi[1], Habiba Almohsen[1]

[1] Mechanical Engineering Department, Higher Colleges of Technology, Abu Dhabi Men's College, Abu Dhabi, UAE

**ARTICLE INFO**

***Article history:***
Received 28 June 2022
Received in revised form 1 July 2022
Accepted 2 July 2022
Available online 31 July 2022

***Keywords:***
Jet impingement; Conduction and convection heat transfer; Nusselt number; Thermal characteristics; volume of fluids

**ABSTRACT**

A numerical study using the conjugate heat transfer approach has been performed to investigate the effects of boundary heat flux, conduction effect, and working fluid on the thermal characteristics due to the jet impingement process. Air and water are used in this study as working fluids. For the water jet, the volume of fluid method is used to capture and track the interface in the multiphase flow. It is found that the wall conduction may change the fluid-solid interfacial thermal characteristics compared with no conduction or pure convection process. The amount of influence depends on the working fluid, nozzle size, metal thermal conductivity, metal thickness, and boundary heat flux. The conduction inside the solid wall tends to reorganize the uniform heat flux distribution at the boundary to a non-uniform heat flux distribution at the fluid-solid interface. This is mainly attributed to the conjugate effect of the solid. For a given jet Reynolds number and boundary heat flux, the conjugate heat transfer results divulge that the convective heat flux removed from the stagnation point is higher for the air jet than for the water jet. Contrary to the air jet, the effect of thermal boundary on the stagnation Nusselt number profile is negligible for the water jet. The disc material and thickness have no obvious effect on the stagnation Nusselt number profile for both air and water fluids.

## 1. Introduction

Impinging jets provide an effective mechanism to transfer energy and mass in various engineering applications ranging from textiles to the cooling of the rocket launcher. Due to its high localized heating and cooling rates, a turbulent jet of gas or liquid directed to the target can efficiently heat up or cool down a specific region. The heat transfer mechanism related to the jet impingement process has been studied, both experimentally and numerically [1-11]. In all earlier studies, the effects of the nozzle diameter, jet Reynolds number, and nozzle-to-target spacing on the thermal characteristics have been adequately investigated. Nevertheless, there are still other aspects that should be inspected to enhance our understanding of the jet impingement process, e.g., conjugate heat transfer, working fluid type, and the effect of the boundary heat flux on the thermal characteristics.

* *Corresponding author.*
*E-mail address: gnasif@hct.ac.ae (Ghassan Nasif)*

https://doi.org/10.37934/cfdl.14.7.1830

Many industrial and engineering applications are exposed to a strong thermal interaction between fluids and solids. Conjugate heat transfer (CHT) is hence a vital subject in the industry, which can be assessed in various methods. Analytical methods produce good results to recognize the main parameters of the problem and verify the codes. However, the applications of the analytical methods are limited to very simple shapes [12-15]. Experiments, which are an alternative means to the analytical methods, are significantly expensive and cannot be completely relied on in the industry. Modern computational CHT was developed after computers came into a wide application to substitute the empirical expressions of proportionality of heat flux to temperature difference with heat transfer coefficient (HTC). The state-of-the-art of computational method includes coupling the conduction in the solid and convection in the fluid to predict the HTC at the interface. The coupled approach is more reliable and more realistic than a decoupled solution [12]. In the computational CHT approach, two separate simulations are created, one for fluid analysis and another for solid thermal analysis. Assuming the temperature distribution on the wall boundary, the fluid flow problem is solved to evaluate the local HTC distribution on the wall. The HTC profile with the reference temperature is applied to the solid thermal simulation to re-evaluate the temperature distribution in the solid. The wall temperature distribution predicted by the solid thermal analysis is fed back to the transient flow simulation and applied as a wall boundary condition to re-evaluate the modified HTC distribution at the interface. The iteration process continues until the solution is obtained with appropriate accuracy.

Tepe *et al.,* [16] investigated experimentally the effect of extended jet holes on the performance of convective heat transfer. The study aims to explain the effect of extended jet holes on the heat transfer performance of the in-line array jet impingement configuration and to eliminate the detrimental effect of cross-flow on heat transfer performance and flow characteristics. The study is conducted by using fully turbulent jet flow impinges on a flat surface. The jet's Reynolds number (Re) ranges between $16250 \leq Re \leq 32500$. It was concluded that the maximum average and local Nu numbers were obtained on the condition of a nozzle diameter to a target gap ratio of 2.0. Lu *et al.,* [17] evaluated numerically the cooling performance of a novel rotary jet impingement system. Parametric studies considering the jet exit Reynolds numbers, the fluid properties, and the rotation speeds were carried out in the study. It was concluded that the increase of the Reynolds number had a direct impact on the heat transfer performance of the jet impingement cooling. Furthermore, the average Nusselt number increases with the increase of the pipe rotational speed. The uniformity of the heat removal performance was enhanced with the increase of the pipe rotational speed. Oliveira *et al.,* [18] investigated the jet impingement process that is used in the metallurgical industry. A cooling set up with a large nickel plate is used as a test sample, which was heated until 850°C before being cooled by a single circular water jet. Five experimental results are presented in the study with different jet Reynolds numbers. The Reynolds number is controlled by varying the water flow rate and the nozzle diameter. They revealed that the increase in the jet Reynolds number increased slightly the convective heat flux at the stagnation zone but increased it substantially for positions farther from the impact location. The change in the nozzle diameter did not significantly affect the heat transfer or the rewetting front growth, although the heat dissipation was slightly higher with the smaller nozzle, possibly because of the higher jet impact velocity.

The objective of the current study is to provide an enhanced picture of the convection mechanism and to evaluate the effect of the CHT process and boundary heat flux on the convective heat transfer coefficient due to the jet impingement process. For this purpose, numerical simulations are carried out using fully developed circular air and water jets, impinging on a heated flat plate of various thicknesses. The thermal results from the simulations are presented and compared for different situations.

## 2. Methodology

In the current study, all cases are simulated using STAR-CCM+ - Siemens PLM commercial code with an unstructured polyhedral mesh. The major advantage of polyhedral cells is that they generally have many neighbors, so gradients of the variable at cell centers can be much better approximated compared to other mesh types. Polyhedrons are also less sensitive to stretching than other mesh types, i.e., tetrahedrons, which results in better mesh quality leading to improved numerical stability of the model. In addition, numerical diffusion is reduced due to mass exchange over numerous faces. This leads to a more accurate solution achieved with a lower cell count [19]. The governing equations for transient analysis include continuity, momentum, and energy equations. Each of these equations can be described in a general way by the transport of a particular scalar quantity $\phi$, represented in a continuous integral form as [20]

$$\frac{\partial}{\partial t}\int_{\mathrm{CV}}^{0}\rho\phi d\mathrm{V}+\oint_{A}^{0}\mathbf{n}.(\rho\phi\mathbf{u})dA=\oint_{A}^{0}\mathbf{n}.\left(\Gamma_{\phi}\boldsymbol{\nabla}\phi\right)dA+\int_{\mathrm{CV}}^{0}S_{\phi}\,d\mathrm{V} \tag{1}$$

Here CV is the control volume, $A$ is the surface area of the control volume, $\mathbf{n}$ is the unit outward normal vector to the surface element $dA$, $\mathbf{u}$ is the velocity vector and $\rho$ is the density. The terms in Eq. (1), from left to right are, the rate of change in the property $\phi$ in the control volume, the rate of change in the property $\phi$ due to the convection flux across the boundaries of the control volume, the rate of change the property $\phi$ due to the diffusive flux across the boundaries of the control volume, and the source term. The source term in Eq. (1) contains the effects of the pressure gradient and all types of body forces. The set of fluid transport equations is obtained by selecting appropriate expressions for the diffusion coefficient $\Gamma_{\phi}$ and source term $S_{\phi}$ and setting the variable $\phi$ in Eq. (1) to velocity vector components for momentum equations, and $\mathrm{i}$ for energy equation, where $\mathrm{i}$ is the internal energy of the fluid or solid. The integral form of the mass conservation equation can also be obtained from Eq. (1) by setting $\phi=1$ and the source term $S_{\phi}=0$.

Two working fluids are used in the current study, i.e., water and air. For the water jet, the flow field in the present study involves two different fluids, i.e., water and air. Therefore, a model to handle two-phase flow is required in the simulations. The volume of fluid (VOF) is a simple and efficient technique that provides an approach to capturing the movement of the interface between the mixture phases [21]. The transport equation for the volume fraction $\alpha_i$ of the $i^{\mathrm{th}}$ fluid phase in the control volume, CV is described in the form of Eq. (1) with no source term, $\phi=\alpha_i$ and $\Gamma_{\phi}=0$ as:

$$\int_{CV}^{0}\frac{\partial\alpha_i}{\partial t}\,d\mathrm{V}+\int_{CV}^{0}\mathbf{u}.\boldsymbol{\nabla}\alpha_i\,d\mathrm{V}=0 \tag{2}$$

The challenging task in the VOF method is to discretize the convective term in Eq. (2) in a way that avoids artificial smearing of the step interface profile due to numerical diffusion. High-resolution schemes are the most efficient approach used to resolve this issue [22-24]. High-Resolution Interface-Capturing (HRIC) is used for capturing the interface with the VOF model in the present study. This scheme relies on the use of a normalized variable diagram, which provides the methodology for constructing high-resolution schemes [25].

In the current study, one of the important requirements of the computational model is to account for the interaction between the impinging jet and the wall to obtain good results for the heat transfer coefficient. The *k-ω* SST model, which has been proven to be more accurate in capturing wall effects than other Reynolds-Averaged Navier-Stokes (RANS) models (STAR-CCM+ - Siemens PLM, User Manual), solves additional transport equations for turbulent kinetic energy *k* and specific dissipation

rate $\omega$, from which the turbulent viscosity $(\mu_t)$ can be derived [26]. The transport equations for $k$ and ω are provided in a study by Versteeg and Malalasekera [20]. A semi-implicit method for pressure-linked equations (SIMPLE) algorithm is used to solve the discretized equations in a segregated manner [20]. In the segregated approach, the discretized equations are treated separately from one another and solved sequentially and iteratively. The segregated fluid temperature model solves the total energy equation with temperature as the independent variable. In this model, the heat flux vector $\mathbf{q}$ in the diffusion term is given as:

$$\mathbf{q} = -\kappa_{eff}\boldsymbol{\nabla}T \tag{3}$$

where $\kappa_{eff}$ is the effective thermal conductivity, given by:

$$\kappa_{eff} = \kappa + \frac{\mu_t c_p}{Pr_t} \tag{4}$$

where $\kappa$, $c_p$ and $Pr_t$ are the thermal conductivity, specific heat capacity, and turbulent Prandtl number, respectively. The main purpose of the turbulent Prandtl number is to calculate the eddy thermal conductivity $(\mu_t c_p/Pr_t)$ after the evaluation of the dynamic eddy viscosity. The turbulent Prandtl number may be evaluated numerically or experimentally and its value ranges between $Pr_t$ = 0.72 - 0.92 (STAR-CCM+ - Siemens PLM, User Manual). The conjugate heat transfer method is used to evaluate the heat transfer coefficient on the fluid-solid interface in a coupled manner. In the conjugate method, an iterative solution is required between solid and fluid for each time step as illustrated earlier in the introduction section.

## 3. Model Setup

This study is a continuation of our previous studies by Nasif *et al.,* [6] and Nasif *et al.,* [27], therefore the same computational domain, boundary conditions, cell-independent study, and the validation process will be utilized from previous studies. Figure 1 shows the computational domain with relevant boundary conditions. Grids independent study was carried out in the earlier stage to select the optimum mesh count. The criteria for choosing the cell count in the current study are based on the validation process, i.e., the numerical results for many grids and many parameter settings were checked and compared with experimental results [27]. Prism layers are clustered at the fluid-solid interface to better resolve the wall effect, producing a dimensionless wall distance value of less than $y+ < 3.0$ at the solid-fluid interface for both working fluids, i.e., water and air. The mesh are clustered at the jet trajectory and also where the wall jet is expected adjacent the wall. First-order implicit time marching and second-order spatial differencing are used to discretize the governing equations, within a finite volume framework. The CHT is used to couple the heat transfer solution between fluid and solid. The time step for the simulations was set at $1\times10^{-3}$ s with twenty internal iterations.

Smooth pipe nozzles with diameters of $d$ = 12.5 and 25.0 mm for air and $d$ = 4.0 and 6.0 mm for water are used to produce a fully developed pipe flow profile. This profile is mapped as a velocity inlet boundary to the computational domain at the nozzle exit as shown in Figure 1. To ensure a fully developed velocity profile, pipes with a length to diameter ratio of $L/d = 50$ are used in separate simulations. A wide range of jet Reynolds number, i.e., Re = 5000 – 30000 with target spacing-to-nozzle of $H/d$ = 6.0 is employed in the simulations.

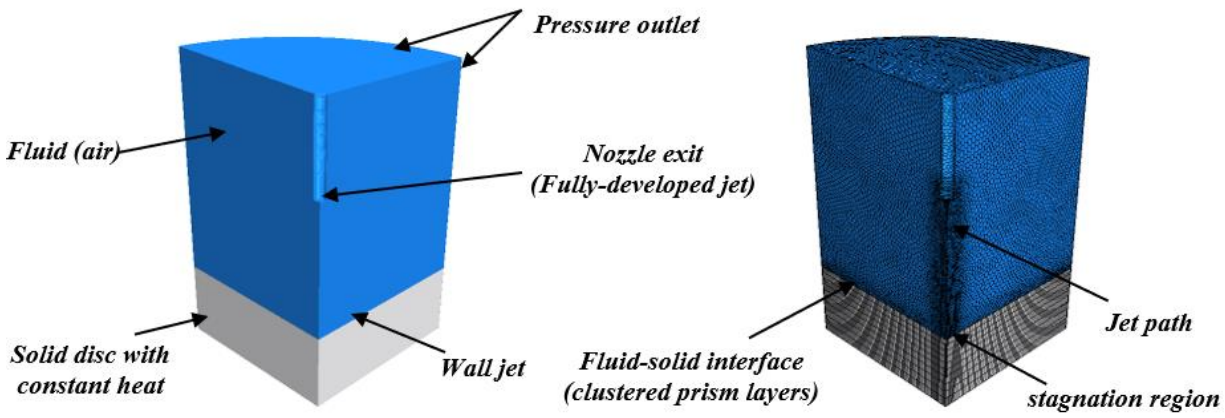


(a) (b)

**Fig. 1.** Computational domain with relevant boundary conditions; (a) Section in the computational domain, (b) Meshed domain (polyhedral cell)

The effect of the thermal boundary, i.e., heat flux strength is initially investigated by using a zero plate thickness of diameter $D$ = 600 mm, while the CHT numerical process is implemented for two different materials with two plate thicknesses, i.e., $t_p$ = 5.0 and 10.0 mm. The thermal properties of plate materials are given in Table 1. The water and air physical properties are evaluated as a function of the local temperature in the computational domain. A range of constant boundary heat flux, i.e., $q_B$ = 500 – 5000 W/m$^2$, is employed as a thermal boundary condition for different cases in the study; the subscript letter *B* is used to represent the bottom face (or boundary) of the disc. The local Nusselt number at the fluid-solid interface is evaluated as [28]:

$$\mathrm{Nu} = \frac{hd}{\kappa_f} \tag{5}$$

where $\kappa_f$ is the thermal conductivity of the jet fluid evaluated at the nozzle exit temperature, *h* is the local heat transfer coefficient calculated from Newton's law of cooling as [28]:

$$h = q_i / \left(T_i - T_{ref}\right) \tag{6}$$

where $q_i$ and $T_i$ are the local heat flux and the local wall temperature at the fluid-solid interface, i.e., the upper face of the disc, and $T_{ref}$ is a reference temperature. The temperature at the nozzle exit is used as the reference temperature to evaluate the heat transfer coefficient in Eq. (6). The jet issuing temperature is $T_{ref} = T_j = 20$°C. The pressure outlet boundaries are used at the top and side portions of the computational domain as shown in Figure 1.

**Table 1**
Physical properties of the investigated metals

| | Density, ρ (kg/m$^3$) | Thermal Conductivity, $\kappa$ (W/m. K) | Specific Heat, $c_P$ (J/kg. K) | Thermal Diffusivity, $\alpha$ (m$^2$/s) |
|---|---|---|---|---|
| Aluminum (Al) | 2702 | 237 | 903 | 1.0E-04 |
| Stainless Steel (316 SST) | 7990 | 15.4 | 500 | 4.0E-06 |

## 4. Validation

Validation is the process used to assess the accuracy and reliability of the computational model and to ensure that the model can predict acceptable results. Validation involves several aspects including proper physical and mathematical representations of the problem, appropriate numerical schemes, and accuracy of the model predictions. Extensive validations are carried out in our previous studies using water and air jets [6-11, 27]. In this section, the validation using the air jet is presented only for brevity [6]. The normalized local Nusselt number from the numerical simulations is compared with experimental data at different radial locations (*r*) from the stagnation region as shown in Figure 2 [2].

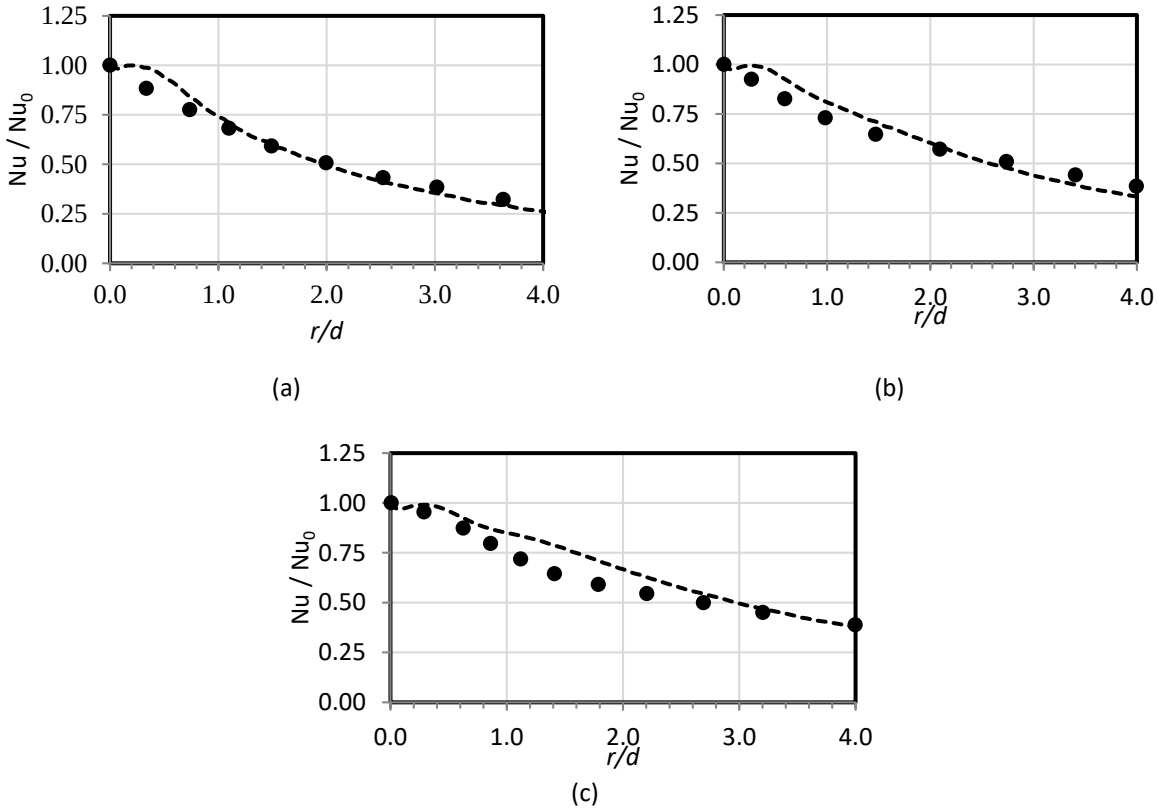


**Fig. 2.** Computational (---) and experimental (••• - [2]) results at *H/d* = 6.0; (a) Re = 5000, (b) Re = 15000, (c) Re = 30000

In Figure 2, the $Nu_0$ and Nu represent the stagnation region and local Nusselt number, respectively. The local Nusselt number (Nu) is normalized using the stagnation Nusselt number ($Nu_0$), while the radial direction is normalized by the diameter of the nozzle. The Nusselt number is calculated based on the nozzle diameter and the air temperature at the nozzle exit, i.e., 20°C. Three jet Reynolds numbers for nozzle diameter of *d* = 25.0 mm and *H/d* = 6.0 are used in the validation process, i.e., Re = 5000, 15000 and 30000. The validation process is performed by neglecting the conjugate effect to mimic the experiment setup, i.e., the jet impinges a flat plate with zero thickness and $q_B$ = 1000 W/m$^2$ [2]. The difference between the computational and experimental results increases with the Reynolds number. It is shown that the computational model can reproduce the experimental data with a maximum difference of less than 10% for Re = 30000. Therefore, the present simulations can satisfactorily predict the heat transfer performance of the impinging jet. The validation process was also performed for the air-jet at *H/d* = 4.0 and 10.0; the results were

comparable to what is shown in Figure 2. More information about the validation process is available in our previous study by Nasif *et al.,* [27].

## 5. Results

The computational results from different flow conditions and thermal parameters that are employed to investigate the effect of the boundary heat flux predicted by the CHT process on the thermal characteristics due to the jet impingement heat transfer are presented for target spacing-to-nozzle of *H/d* = 6.0 in this section.

Figure 3 shows the effect of the jet Reynold number on the stagnation point Nusselt number ($Nu_0$). As shown in this figure and for a given jet Reynolds number, the HTC at the stagnation point increases as the nozzle size decreases, while for a given nozzle size, it increases with the Reynolds number. In Figure 3, two heat fluxes are used as boundary conditions to investigate the effect of the thermal boundary on the stagnation HTC. The $\mathrm{Nu}_0$ is obtained by using the corresponding nozzle size and fluid thermal conductivity at the nozzle exit. It is obvious in Figure 3 that the $\mathrm{Nu}_0$ profile is only a function of the jet Reynolds number when the size of the nozzle is large for both air (*d* = 25.0 mm) and water (*d* = 6.0 mm) jets. Therefore, the boundary heat flux has no effect on the $\mathrm{Nu}_0$ profiles when the size of the nozzle is large (see blue and black dotted lines in Figure 3). For smaller nozzles sizes, the dependence of the $\mathrm{Nu}_0$ profile on the thermal boundary is more obvious for the air jet (*d* = 12.5 mm) rather than the water jet (*d* = 4.0 mm). As the boundary heat flux increases, the $\mathrm{Nu}_0$ profile is shifted upwards for small nozzles with the increase of the jet Reynolds number. Therefore, a correlation to predict the $\mathrm{Nu}_0$ profile can be easily set up over a wide range of Reynolds number for the water jet. The results from experiments for zero plate thickness is also presented in Figure 3, which provides further validation for the simulations that are used in the present study. The maximum difference between experimental and computational $\mathrm{Nu}_0$ is less than 8%, which occurs with the water jet for $d = 6.0$ mm.

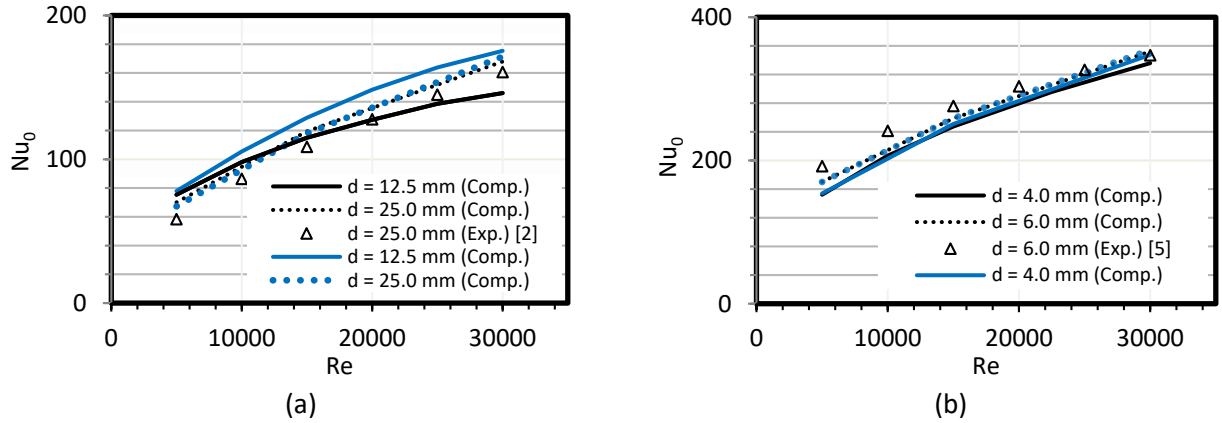


Black lines: $q_B$= 1000 W/m$^2$; Blue lines: $q_B$= 5000 W/m$^2$

**Fig. 3.** Effect of the jet Reynolds number on the stagnation point Nusselt number; (a) air jet, (b) water jet

The effect of the boundary heat flux ($q_B$) on the nondimensional local heat transfer coefficient ($\mathrm{Nu}$) is examined using three jet Reynolds numbers as shown in Figure 4. In this figure, the normalized Nusselt number ($\mathrm{Nu}/\mathrm{Nu}_0$) is plotted against the normalized radial distance ($r/d$) from the stagnation point for various cases.

Several conclusions can be inferred from Figure 4: (1) The ($\mathrm{Nu}/\mathrm{Nu}_0$) profile for the smaller nozzle with the air jet (blue lines in Figure 4(a), Figure 4(b), and Figure 4(c)) is more sensitive to the thermal

boundary compared to the larger sized nozzle (black lines) where the $(\mathrm{Nu}/\mathrm{Nu}_0)$ profile is a function of only $r/d$ for all heat fluxes that are used in the simulations. For nozzle diameter $d = 12.5$ mm, the profile is, to some extent, a function of both the radial distance and thermal boundary as the $(\mathrm{Nu}/\mathrm{Nu}_0)$ profile with the heat flux $q_B$= 1000 W/m$^2$ is slightly shifted above the one of $q_B$= 5000 W/m$^2$; (2) The $(\mathrm{Nu}/\mathrm{Nu}_0)$ profiles for both air nozzles are shifted up at downstream radial locations from the stagnation point as the jet Reynolds number increases. This reveals that the local $\mathrm{Nu}$ enhances with the jet Reynolds number due to the decrease of the surface temperature at downstream locations [27]; (3) The $(\mathrm{Nu}/\mathrm{Nu}_0)$ profile for the water jets is a function of $r/d$ only and it is independent of the nozzle size and boundary heat flux when the jet Reynolds number is small as shown in Figure 4(d). Nevertheless, the $(\mathrm{Nu}/\mathrm{Nu}_0)$ profile for the water jet becomes more sensitive to the nozzle size and boundary heat flux as the jet Reynolds number increases as shown in Figure 4(e) and Figure 4(f). For a given nozzle size, the $\mathrm{Nu}/\mathrm{Nu}_0$ profile is shifted upwards as the boundary heat flux increases, while for a given heat flux, the profile is shifted upwards as the nozzle size increases as shown in Figure 4(f). At Re = 15000, the deviation in the $\mathrm{Nu}/\mathrm{Nu}_0$ profiles are clearer for the smaller nozzle rather than the larger size nozzle as shown in Figure 4(e), which reveals that the smaller nozzle is more sensitive to the boundary heat flux at a medium-ranged jet Reynolds number; (4) As in the air jet, the $\mathrm{Nu}/\mathrm{Nu}_0$ profile for the water jet is shifted up at downstream positions as the jet Reynolds number increases. From the above conclusions and upon close examination of Figure 4, one can conclude that a correlation to anticipate the $\mathrm{Nu}/\mathrm{Nu}_0$ profile for a broad range of boundary heat fluxes can be set up with appropriate accuracy for the air and water jets cases that are given in Figure 4(a) to Figure 4(e). This correlation is a function of only $r/d$ for any given jet Reynolds number.

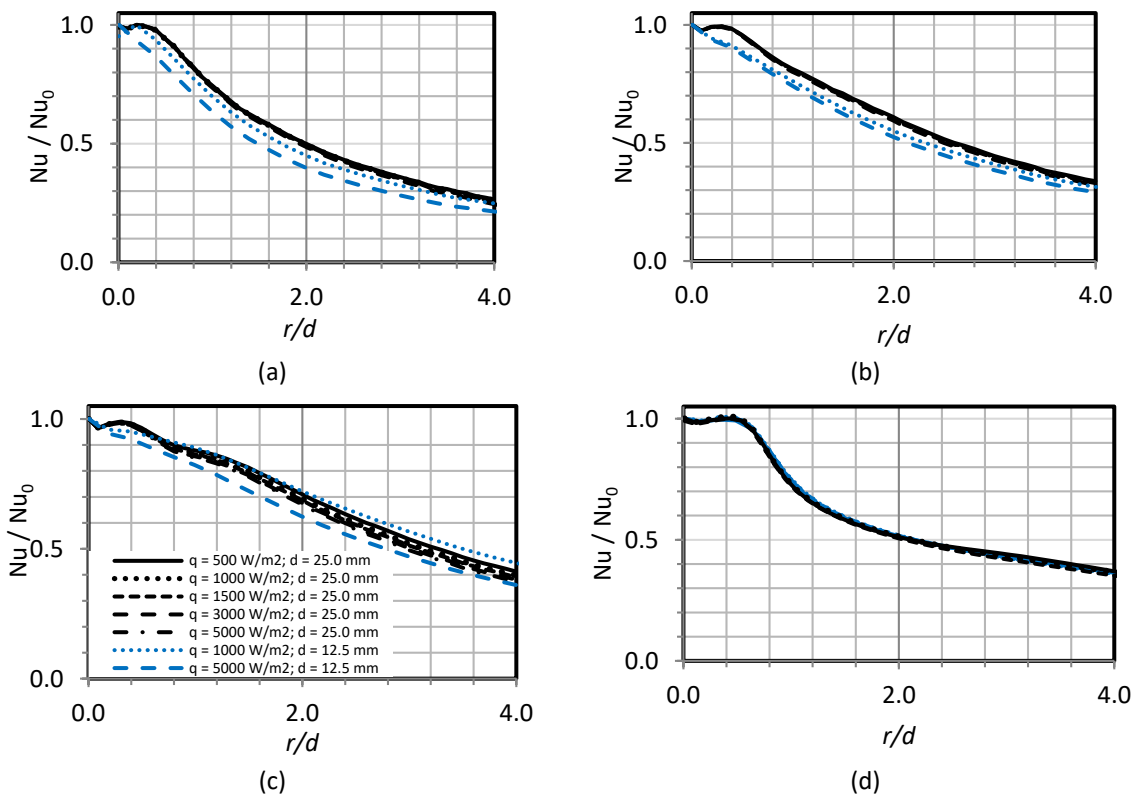

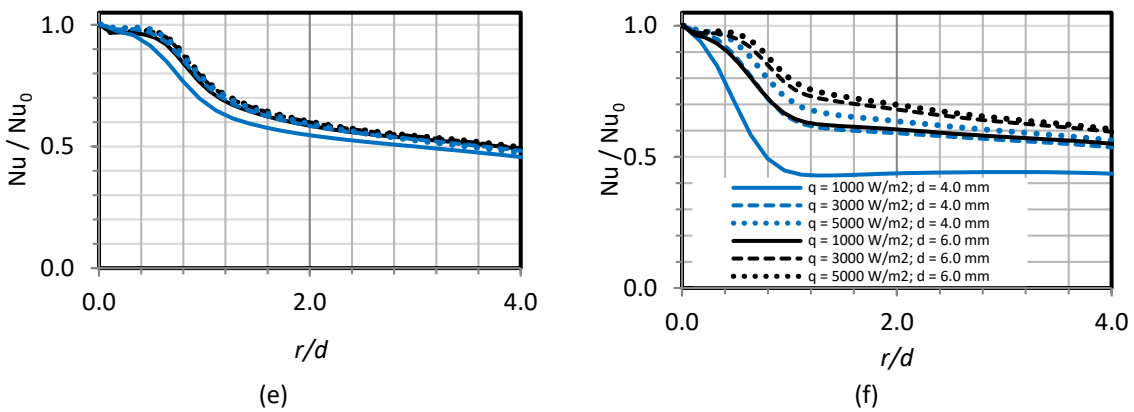


(e) (f)

Black lines: d = 25.0 mm (air) or 6.0 mm (water); Blue lines: d = 12.5 mm (air) or 4.0 mm (water)

**Fig. 4.** Effect of thermal boundary strength on the $\mathrm{Nu}/\mathrm{Nu}_0$ profile for air and water jets; (a) Air Jet - Re = 5000, (b) Air Jet - Re = 15000, (c) Air Jet - Re = 30000, (d) Water Jet - Re = 5000, (e) Water Jet - Re = 15000, (f) Water Jet - Re = 30000

The above discussion was intended to investigate the thermal characteristics of the jet impingement onto a plate with a thickness of zero, where the conductive heat resistance in the radial direction $R_{tr}$ is infinity. Therefore, there is no conductive heat transfer in the radial direction but pure convection heat transfer in the axial direction. When the solid plate has a finite thickness, the conductive heat transfer inside the solid has a significant role in the convective heat transfer from the plate surface. The conductive heat transfer process will act to readjust the uniform boundary heat flux inside the solid and make a change not only at stagnation but also in the local Nusselt number [29]. As the plate thickness increases, the thermal resistance in the transverse direction ($R_{tr} \propto \frac{1}{\kappa.t_p}$) decreases, while the thermal resistance in the axial or normal direction ($R_a \propto \frac{t_p}{\kappa}$) increases. Therefore, the conductive heat transfer in the radial direction towards the impingement point, which acts as a heat sink increases with the plate thickness, while the axial conductive heat transfer towards the fluid-solid interface decrease as the plate thickness increases. The boundary heat flux will not stay uniform at the interface as in the case of the zero plate thickness. In the convective heat transfer problem that also involves heat conduction in the solid plate, the HTC profile at the interface depends on the thermal properties and thickness of the plate beside the other flow parameters. The effect of wall conduction on the stagnation and local Nusselt number is investigated in this study using the CHT method, for various jet Reynolds numbers and different boundary heat fluxes. The physical properties of the material under investigation are given in Table 1.

Figure 5 shows the effect of the flux strength on the stagnation Nusselt number profile, based on the CHT expectations. The $\mathrm{Nu}_0$ in this figure is evaluated based on the nozzle size and fluid physical properties at the nozzle exit. For all cases that are used in the simulations, the smaller nozzle offers an enhanced convective heat transfer coefficient at the stagnation point (not normalized heat transfer coefficient, i.e., $\mathrm{Nu}_0$). This is attributed to the higher radial velocity gradient and wall shear stress that is associated with the smaller-sized nozzle for a given working fluid [27]. It is obviously seen in Figure 5(a) and Figure 5(b) for the air-cooling jet that the CHT $\mathrm{Nu}_0$ values always decline as the flux strength increases. The rise of the boundary heat flux acts to increase the minimum temperature ($T_0$) and the convective heat transfer ($q_0$) at the stagnation point [6]. However, the increase in $T_0$ is prevailing over the increase in $q_0$. The combined effect acts to reduce the $\mathrm{Nu}_0$ as the boundary heat flux increases. Both the disc material and thickness influence the $\mathrm{Nu}_0$ profile in air jets as shown in Figure 5(a) and Figure 5(b). The disc thickness effect is more apparent for the larger-sized nozzle i.e., *d* = 25.0 mm, rather than for the smaller one. The conduction heat transfer also acts to

reduce the $Nu_0$ value below that of a zero-thickness surface for a wide range of heat fluxes when the size of the nozzle is small as shown in Figure 5(b). Nevertheless, as the nozzle size increases, the CHT process may indicate an increase in the $Nu_0$ value relative to the one without the CHT. The degree of improvement or reduction depends on the disc metal, thickness, and boundary heat flux as shown in Figure 5(a). The maximum $Nu_0$ value for the air-cooling jet that involves a CHT appears with the metal with a lower thermal conductivity, i.e., 316SST, for both nozzle sizes as shown in Figure 5(a) and Figure 5(b). In Figure 5(a), the maximum $Nu_0$ value happens with a disc thickness of $t_p$= 10.0 mm and nozzle size of *d* = 25.0 mm, while it occurs with the disc thickness of $t_p$= 5.0 mm and nozzle size of *d* = 12.5 mm in Figure 5(b). This indicates that for a given flux strength, the nozzle size and CHT implementation together affect the $Nu_0$ value. Contrary to the air jets, the effect of the thermal boundary on the $Nu_0$ profile is minor for the water jet as shown in Figure 5(c) and Figure 5(d). The $Nu_0$ value seems to be constant over a wide range of boundary heat flux. The disc material and thickness have no obvious effect on the $Nu_0$ profile, mainly for the large-sized nozzle, i.e., *d* = 6.0 mm as shown in Figure 5(c). However, the constant $Nu_0$ with the water jets does not mean that the convective heat transfer and temperature at the stagnation point are the same for all cases. It indicates that the change in $q_0$ and $T_0$ at the stagnation point are consistent for any disc thickness and material to produce a constant $Nu_0$.

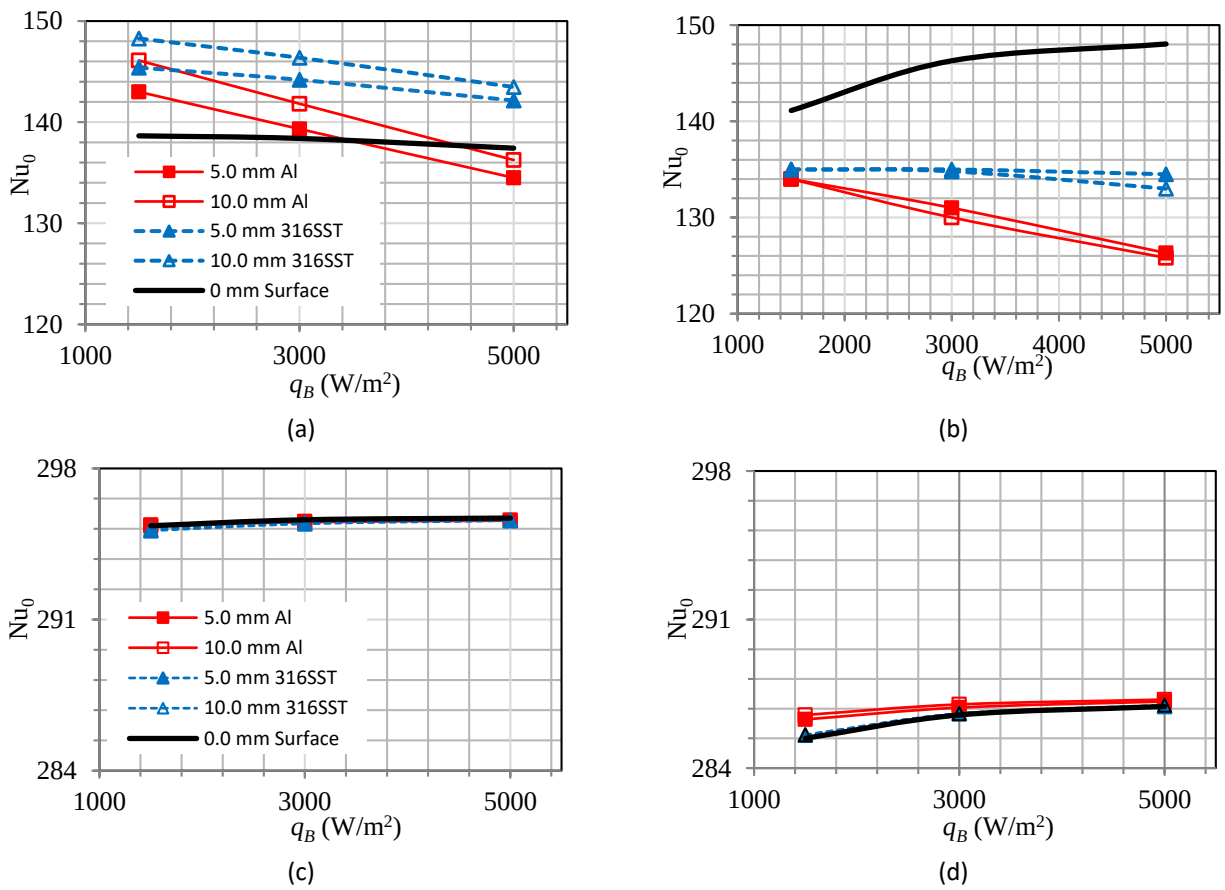


**Fig. 5.** Effect of the boundary heat flux on the $Nu_0$ for the air and water jets; (a) d = 25.0 mm - Air Jet, (b) d = 12.5 mm - Air Jet, (c) d = 6.0 mm - Water Jet, (d) d = 4.0 mm - Water Jet

## 6. Conclusions

A numerical transient study, using the conjugate heat transfer technique for the coupling at the fluid-solid interface, was performed to investigate the effect of the conduction heat transfer in solid, boundary heat flux, and working fluid on the thermal characteristics of jet impingement heat transfer. Two working fluids are used in this study, i.e., air and water, to evaluate the thermal characteristics of the jet impingement process. The volume of fluid (VOF) method is used to capture the air-water interface for the water jet impingement. The conclusions from this study can be briefed as follows:

I. For the pure convection process, the boundary heat flux does not influence on the $\mathrm{Nu}_0$ profiles when the size of the nozzle is large for both air and water jets. However, the dependency of the $\mathrm{Nu}_0$ profile on the thermal boundary is clearer for the air jet rather than the water jet when the size of the nozzle is small.
II. In the absence of conduction with the air jet, the $(\mathrm{Nu}/\mathrm{Nu}_0)$ profile for the smaller nozzle is more sensitive to the boundary heat flux rather than the larger nozzle. The $(\mathrm{Nu}/\mathrm{Nu}_0)$ profile is a function of $r/d$ only when the size of the nozzle is large.
III. The profile of $(\mathrm{Nu}/\mathrm{Nu}_0)$ is a function of $r/d$ only with the water jet in pure convection and it is independent of the nozzle size and boundary heat flux when the jet Reynolds number is small. The profile becomes more sensitive to the nozzle size and boundary heat flux as the jet Reynolds number increases.
IV. The $\mathrm{Nu}_0$ values associated with the air jet case decrease as the boundary heat flux increases. The disc thickness and material affect the $\mathrm{Nu}_0$ profile. On the contrary, the effect of thermal boundary on $\mathrm{Nu}_0$ profile is negligible for the water jet. The disc material and thickness have no obvious effect on the $\mathrm{Nu}_0$ profile.
V. The numerical results indicate that the convective heat flux from the stagnation region is higher for the air jet than that for the water jet for a given operating condition.
VI. The conduction in the solid wall impacts the normalized local heat transfer coefficient for the air jet. The amount of influence depends on the radial location from the stagnation point, metal thickness, thermal conductivity, nozzle size, and the boundary heat flux.
VII. The normalized local heat transfer coefficient profile is insensitive to the conduction in the wall and boundary heat flux for the water jet with the larger nozzle. However, the profile is sensitive to the metal thermal conductivity, thickness, and boundary heat flux for the water jet with the smaller nozzle.

**Acknowledgement**
This work was funded by a Seed grant from Higher Colleges of Technology under Directive (27)/2021. Also, this research was made possible by the facilities of the Shared Hierarchical Academic Computing Network and Compute/Calcul Canada.

## References

[1] Ichimiya, Koichi, Shoichi Takema, Shunichi Morimoto, Tomoaki Kunugi, and Norio Akino. "Movement of impingement heat transfer by a single circular jet with a confined wall." *International Journal of Heat and Mass Transfer* 44, no. 16 (2001): 3095-3102. https://doi.org/10.1016/S0017-9310(00)00341-0
[2] Lee, Jungho Lee, Sang-Joon. "Stagnation region heat transfer of a turbulent axisymmetric jet impingement." *Experimental Heat Transfer* 12, no. 2 (1999): 137-156. https://doi.org/10.1080/089161599269753
[3] Liu, Xin, L. A. Gabour, and J. H. Lienhard. "Stagnation-point heat transfer during impingement of laminar liquid jets: analysis including surface tension." *Journal of Heat Transfer* 115, no. 1 (1993): 99-105. https://doi.org/10.1115/1.2910677

[4] Liu, X., J. H. Lienhard, and J. S. Lombara. "Convective heat transfer by impingement of circular liquid jets." *Journal of Heat Transfer* 113, no. 3 (1991): 571-582. https://doi.org/10.1115/1.2910604
[5] Stevens, J., and Brent W. Webb. "Local heat transfer coefficients under an axisymmetric, single-phase liquid jet." *Journal of Heat Transfer* 113, no. 1 (1991): 71-78. https://doi.org/10.1115/1.2910554
[6] Nasif, Ghassan, and Yasser El-Okda. "Conjugate Effect on the Thermal Characteristics of Air Impinging Jet." *CFD Letters* 13, no. 10 (2021): 25-35. https://doi.org/10.37934/cfdl.13.10.2535
[7] Nasif, G., R. M. Barron, and R. Balachandar. "Numerical simulation of piston cooling with oil jet impingement." *Journal of Heat Transfer* 138, no. 12 (2016). https://doi.org/10.1115/1.4034162
[8] Nasif, Gus, Ram Balachandar, and Ronald M. Barron. "CFD analysis of heat transfer due to jet impingement onto a heated disc bounded by a cylindrical wall." *Heat Transfer Engineering* 37, no. 17 (2016): 1507-1520. https://doi.org/10.1080/01457632.2016.1145021
[9] Nasif, G., R. M. Barron, and R. Balachandar. "Heat transfer due to an impinging jet in a confined space." *Journal of Heat Transfer* 136, no. 11 (2014). https://doi.org/10.1115/1.4028242
[10] Nasif, Ghassan Gus. "CFD Simulation of Oil Jets with Application to Piston Cooling." *PhD diss., University of Windsor, Windsor, Ontario, Canada* (2014).
[11] Nasif, G., R. M. Barron, and R. Balachandar. "Numerical simulation of piston cooling with oil jet impingement." *Journal of Heat Transfer* 138, no. 12 (2016). https://doi.org/10.1115/1.4034162
[12] Radenac, Emmanuel, Jérémie Gressier, and Pierre Millan. "Methodology of numerical coupling for transient conjugate heat transfer." *Computers & Fluids* 100 (2014): 95-107. https://doi.org/10.1016/j.compfluid.2014.05.006
[13] Pozzi, Amilcare, and Renato Tognaccini. "Time singularities in conjugated thermo-fluid-dynamic phenomena." *Journal of Fluid Mechanics* 538 (2005): 361-376. https://doi.org/10.1017/S002211200500529X
[14] Pozzi, Amilcare, and Renato Tognaccini. "Coupling of conduction and convection past an impulsively started semi-infinite flat plate." *International Journal of Heat and Mass Transfer* 43, no. 7 (2000): 1121-1131. https://doi.org/10.1016/S0017-9310(99)00210-0
[15] Fourcher, B., and K. Mansouri. "An approximate analytical solution to the Graetz problem with periodic inlet temperature." *International Journal of Heat and Fluid Flow* 18, no. 2 (1997): 229-235. https://doi.org/10.1016/S0142-727X(96)00089-6
[16] Tepe, Ahmet Ümit, Yaşar Yetişken, Ünal Uysal, and Kamil Arslan. "Experimental and numerical investigation of jet impingement cooling using extended jet holes." *International Journal of Heat and Mass Transfer* 158 (2020): 119945. https://doi.org/10.1016/j.ijheatmasstransfer.2020.119945
[17] Lu, Qi, Rajesram Muthukumar, Haiwen Ge, and Siva Parameswaran. "Numerical study of a rotating liquid jet impingement cooling system." *International Journal of Heat and Mass Transfer* 163 (2020): 120446. https://doi.org/10.1016/j.ijheatmasstransfer.2020.120446
[18] Oliveira, A. V. S., D. Maréchal, J-L. Borean, V. Schick, J. Teixeira, S. Denis, and M. Gradeck. "Experimental study of the heat transfer of single-jet impingement cooling onto a large heated plate near industrial conditions." *International Journal of Heat and Mass Transfer* 184 (2022): 121998. https://doi.org/10.1016/j.ijheatmasstransfer.2021.121998
[19] Sosnowski, Marcin, Jaroslaw Krzywanski, Karolina Grabowska, and Renata Gnatowska. "Polyhedral meshing in numerical analysis of conjugate heat transfer." In *EPJ Web of Conferences*, vol. 180, p. 02096. EDP Sciences, 2018. https://doi.org/10.1051/epjconf/201818002096
[20] Versteeg, Henk Kaarle, and Weeratunge Malalasekera. *An introduction to computational fluid dynamics: the finite volume method*. Pearson Education, 2007.
[21] Hirt, Cyril W., and Billy D. Nichols. "Volume of fluid (VOF) method for the dynamics of free boundaries." *Journal of Computational Physics* 39, no. 1 (1981): 201-225. https://doi.org/10.1016/0021-9991(81)90145-5
[22] Ubbink, O., and R. I. Issa. "A method for capturing sharp fluid interfaces on arbitrary meshes." *Journal of Computational Physics* 153, no. 1 (1999): 26-50. https://doi.org/10.1006/jcph.1999.6276
[23] Muzaferija, Samir. "A two-fluid Navier-Stokes solver to simulate water entry." In *Proceedings of 22nd Symposium on Naval Architecture*, 1999, pp. 638-651. National Academy Press, 1999.
[24] Wacławczyk, Tomasz, and Tadeusz Koronowicz. "Comparison of CICSAM and HRIC high-resolution schemes for interface capturing." *Journal of Theoretical and Applied Mechanics* 46 (2008): 325-345.
[25] Leonard, B. P. "The ULTIMATE conservative difference scheme applied to unsteady one-dimensional advection." *Computer Methods in Applied Mechanics and Engineering* 88, no. 1 (1991): 17-74. https://doi.org/10.1016/0045-7825(91)90232-U
[26] Menter, Florian R. "Two-equation eddy-viscosity turbulence models for engineering applications." *AIAA Journal* 32, no. 8 (1994): 1598-1605. https://doi.org/10.2514/3.12149

[27] Nasif, G., R. Balachandar, and R. M. Barron. "Conjugate analysis of wall conduction effects on the thermal characteristics of impinging jets." *International Journal of Heat and Mass Transfer* 116 (2018): 259-272. https://doi.org/10.1016/j.ijheatmasstransfer.2017.09.034

[28] Çengel, Yunus A., and Afshin Jahanshahi Ghajar. *Heat and Mass Transfer: Fundamentals & Applications*. McGraw-Hill, 2011.

[29] Zhu, Xiao Wei, Lei Zhu, and Jing Quan Zhao. "An in-depth analysis of conjugate heat transfer process of impingement jet." *International Journal of Heat and Mass Transfer* 104 (2017): 1259-1267. https://doi.org/10.1016/j.ijheatmasstransfer.2016.09.075